potential measurements on silica capillaries[20], but somewhat higher than those obtained by Horn *et al.*[4] from force measurement on large silica sheets. In the latter case, however, the silica showed an advancing contact angle of 45°, indicating a lower density of surface silanol groups than for the hydrophilic silica used in our experiments.

At smaller separations, the force predicted by DLVO theory depends on the choice of boundary condition for the surface charge. Our measurements lie between the limits of constant charge and constant potential, but for clarity, only the theoretical interaction at constant potential has been shown in Fig. 2. At very small separations (2–3 nm) DLVO theory predicts that the attractive van der Waals component will exceed the double-layer force, but the measured force is greater than even the limit of constant charge. This effect has been seen previously, and has been attributed to hydration forces[3–6]. In our case, however, the roughness of the substrates complicates analysis of short-range forces.

Variation between the results of surface-potential measurements for different samples illustrates the advantage of force measurements on the actual particles of interest. Minor differences in surface composition or morphology can have a large effect on particle–particle interactions, so it is an advantage to be able to investigate a particle rather than a model system. Although the force measurements presented here agree well with those obtained from macroscopic systems, there may be differences in the interaction forces when pairs of macroscopic or colloid particles interact. For example, because hydrodynamic forces (on a particle approaching a surface) scale with the square of particle radius[21], it is much easier, and of more relevance, to test the influence of relaxation times for surface forces on small particles than on macroscopic systems.

The leading technique for the measurement of surface forces is currently the apparatus of Israelachvili and Adams[7,22]. In that technique the force is measured between a limited number of macroscopic surfaces in crossed cylinder geometry. In contrast, use of a colloid probe allows investigation of particulate and fibrous materials. Particles in the mineral processing and ceramics industries, colloid polymer industries and in biological systems can now be studied directly. □

Received 19 March; accepted 23 July 1991.

1. Derjaguin, B. & Landau, L. *Acta Physiochem.* **14,** 633 (1941).
2. Verwey, E. G. W. & Overbeck, J. J. G. *Theory of the Stability of Lyophobic Colloids* (Elsevier, Amsterdam, 1948).
3. *Proc. Nobel Conf. Hydration Forces and Molecular Aspects of Solvation Chem. Scr.* **25,** 3–31 (1985).
4. Horn, R. G., Smith, D. T. & Haller, W. *Chem. Phys. Lett.* **162,** 404–408 (1989).
5. Rabinovich, I., Derjaguin, B. V. & Churaev, N. V. *Adv. Colloid Interf. Sci.* **16,** 63–78 (1982).
6. Peschel, G., Belouschek, P., Muller, M. M., Muller, M. R. & Konig, R. *Colloid Polym. Sci.* **260,** 444–451 (1982).
7. Israelachvili, J. N. & Adams, G. E. *JCS Faraday Trans. I* **74,** 975–1001 (1978).
8. Horn, R. G. & Israelachvili, J. N. *Chem. Phys. Lett.* **71,** 192–194 (1980).
9. Pashley, R. M. *J. Colloid Interf. Sci.* **83,** 531–546 (1981).
10. Pashley, R. M., McGuiggan, P. M., Ninham, B. W. & Evans, D. F. *Science* **229,** 1088–1089 (1985).
11. Ottewill, R. H. *Concentrated Dispersions* in *Colloid Dispersions* Ch. 9 (ed. Goodwin, J. W.) (Royal Society of Chemistry, London, 1982).
12. Ellmelech, M. *JCS Faraday Trans. I* **86,** 1623–1624 (1990).
Zhenge, X. & Yoon, R. *J. Colloid Interf. Sci.* **134,** 427–434 (1990).
13. Brown, M. A. & Staples, E. J. *Langmuir* **6,** 1260–1265 (1990).
Prieve, D C. & Freij, N. A. *Langmuir* **6,** 396–403 (1990).
14. Binnig, G. & Rohrer, H. *Helv. Phys. Acta* **55,** 726–735 (1982).
15. Binnig, G., Quate, C. F. & Gerber, C. *Phys. Rev. Lett.* **56,** 930–933 (1986).
16. Martin, Y., Williams, C. & Wickramasinghe, H. *J. appl. Phys.* **61,** 4223–4229 (1987).
17. Burnham, N. A. & Colten, R. J. *J. Vac. Sci. Technol.* **A7,** 2906–2913 (1989).
18. Ducker, W. A. & Cook, R. F. *Appl. Phys. Lett.* **56,** 2048–2410 (1990).
19. Weisenhorn, A. L., Hansma, P. K., Albrecht, T. R. & Quate, C. F. *Appl. Phys. Lett.* **54,** 2691–2653 (1989).
20. Wiese, G. R., James, R. O. & Healy, T. W. *Disc. Faraday Soc.* **52,** 302–311 (1975).
21. Chan, D. Y. C. & Horn, R. G. *J. chem. Phys.* **83,** 5311–5324 (1990).
22. Parker, J. L., Christenson, H. K. & Ninham, B. W. *Rev. sci. Instrum.* **60,** 3135–3138 (1989).
23. Meyer, G. & Amer, N. M. *Appl. Phys. Lett.* **53,** 1045–1047 (1988).
24. Derjaguin, B. V. *Kolloid. Zh.* **69,** 155–164 (1934).
25. Hunter, R. J. *Foundations of Colloid Science,* 222 (Clarendon, Oxford, 1987).
26. Chan, D. Y. C., Pashley, R. M. & White, L. R. *J. Coll. Inter. Sci.* **77,** 283 (1980).

ACKNOWLEDGEMENTS. We thank B. W. Ninham for support, J. Parker for the use of his plasma reactor, T. Nylander for providing the oxidized wafer, and C. Drummond and T. W. Healy for discussions.

Dimension of weather and climate attractors

Edward N. Lorenz*

Institute for Nonlinear Science, University of California at San Diego, La Jolla, California 92093, USA
* Present address: Department of Earth, Atmospheric, and Planetary Sciences, Massachusetts Institute of Technology, Cambridge, Massachusetts 02139, USA

A PROCEDURE for estimating the correlation dimension of the attractor of a dynamical system[1] has been applied to a number of data sets that are representative of weather or climate variations. Reported values of the attractor dimension have typically fallen between 3.0 and 8.0 (refs 2–9). Because the atmosphere is so complex, these values have seemed surprisingly low, and doubts as to their appropriateness have been expressed even by the originators of the method[8,10,11]. Here I apply the procedure to 'data' generated by a mathematical system whose dimension can be evaluated by other means, and identify conditions, apparently satisfied by the studies that use real data, in which the procedure will yield systematic underestimates. It therefore seems unlikely that global weather or climate systems possess low-dimensional attractors.

The quantities selected for analysis have included sea-level pressures[2], upper-level geopotential heights[3,4], low-level vertical velocity components[5], rainfall intensities[6], sunshine durations[2], cyclone positions[7], large-scale wave amplitudes[2], tree-ring widths[8] and oxygen-isotope concentrations in deep-sea cores[2,8,9]. The findings have raised hopes that suitably constructed models with relatively few variables might recapture the dynamics of the weather or the climate.

In a typical study one begins with an extensive sequence of values of a single scalar quantity $x(t)$, observed at equally spaced times t. The corresponding sequence of vectors $[x(t), y(t), \ldots]$, where $y(t), \ldots$ are other scalar quantities coupled to $x(t)$, constitutes a sample of a dynamical system, but in general the values of $y(t), \ldots$ are not known. One therefore attempts to reconstruct the system by choosing a time lag τ and an embedding dimension

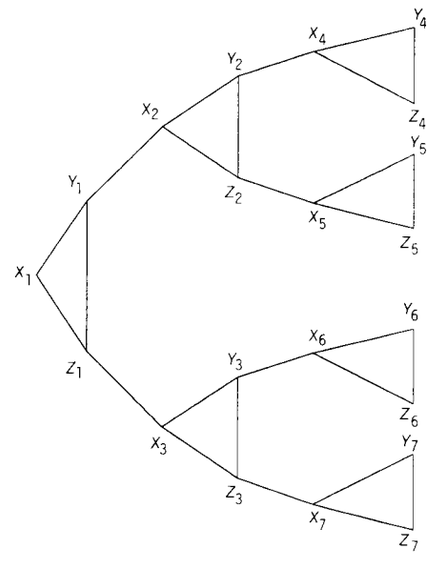

FIG. 1 Coupling scheme for variables in equation (1) with $L = 3$. Line segments forming sides of triangles represent strong nonlinear coupling between variables with like subscripts; segments connecting triangles represent weak or strong linear coupling between variables with different subscripts.

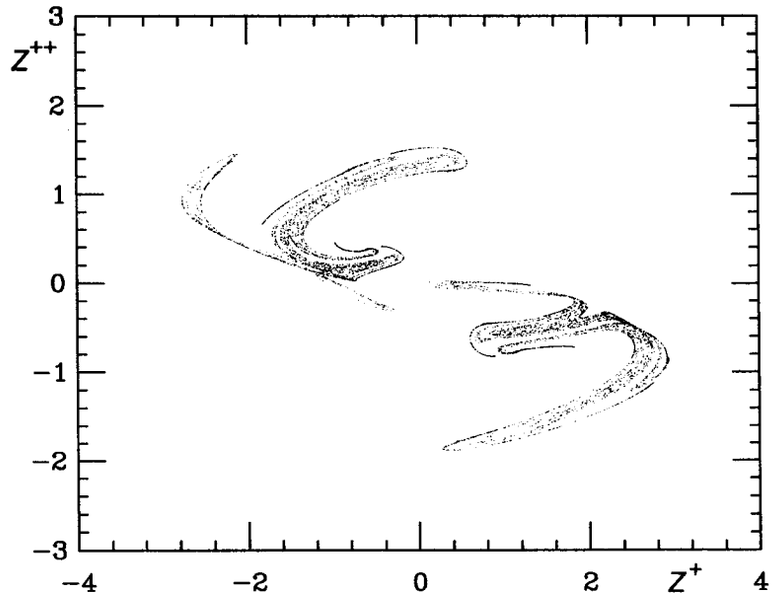

FIG. 2 Poincaré section of reconstructed attractor of equation (1) with $L=1$, obtained by plotting $Z^{++}=Z_1(t'+2\tau)$ against $Z^{+}=Z_1(t'+\tau)$ for times when $Z_1(t')=0$.

n, and forming the vectors $[x(t), x(t+\tau), \ldots, x(t+n\tau-\tau)]$ for N times t spaced at intervals τ'; sometimes $\tau'=\tau$. Finally one determines by direct count, for various values of r, the number $m(r)$ of pairs of vectors whose vector difference is less than r in magnitude. If, as r approaches zero, $m(r)$ varies as $r^{d(n)}$, the estimated correlation dimension of the attractor of the reconstructed system is $d(n)$. If, as n is successively increased, $d(n)$ approaches a limit d_c, the estimated correlation dimension of the attractor of the original system is d_c.

A number of factors that might produce misleading results have been noted[12,13]; some of them can be overcome by simple modifications. Here I propose another explanation for the seemingly low estimates.

A key phrase in defining d_c is 'as r approaches zero.' As pointed out by Ruelle[14], unless N is very large the smallest value of r for which $m(r)$ is large enough to be statistically meaningful may not be particularly close to zero. If, for example, $N=4{,}000$, and if in reality $d_c=8.0$, $m(r)$ can decrease all the way from its maximum, about 8×10^6, to unity while r decreases by a factor of less than eight.

In concluding that d_c is small, then, the investigators have implicitly assumed that the fine structure of the attractor would, on magnification, resemble the coarse structure, so that, if N were made large enough, the decrease of $m(r)$ with r when r is very small would be like that when r is fairly large. Although this is demonstrably the case for some simple systems, it need not be so for more intricate ones, including some in which certain subsets of the variables are only weakly coupled to others. In the atmosphere much of the coupling is weak and indirect. If convective-cloud circulations over London and Washington, for example, can affect each other at all, they can do so only by being coupled to the general weather patterns in their own neighbourhoods, which may in turn be coupled to the same globe-encircling westerly wind current. I propose that if the variable selected for analysis is strongly coupled to only a few variables of the system, the estimated value of d_c, if N is only moderately large, will be considerably less than the dimension as determined by other standard methods, such as the Kaplan–Yorke[15] formula.

I have arrived at this hypothesis after studying special cases of a model with $(3\times(2^L-1))$ variables, with $L=1$ or $L=3$, where the Kaplan–Yorke dimension d' may be readily estimated. The model was formed by taking 2^L-1 copies of a three-variable model whose properties I had previously studied in detail[16],

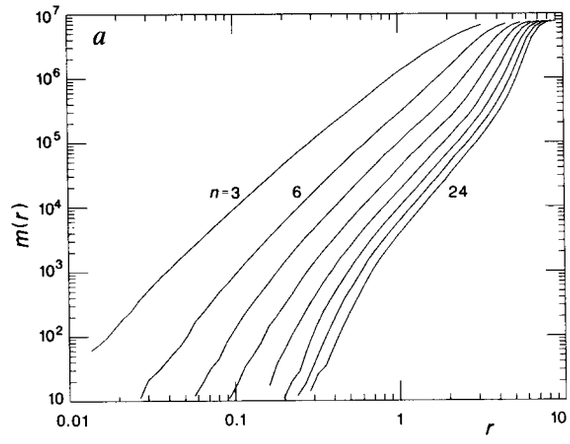

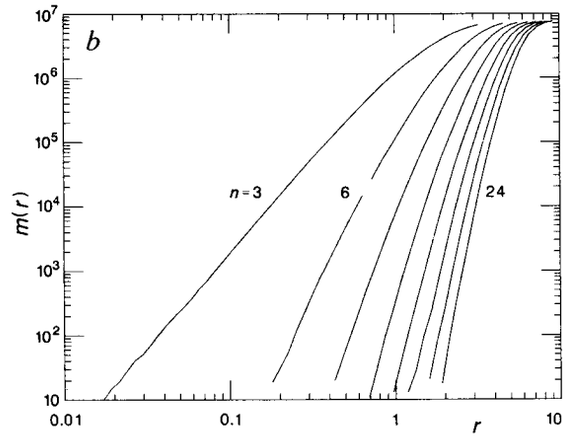

FIG. 3 *a*, Curves of $m(r)$ against r for embedding dimensions $3, 6, \ldots, 24$, obtained by applying GP procedure to equation (1) with $L=3$ and $c=0.1$ and Z_7 as the selected variable. Points plotted for values of $\log_{10} r$ at intervals of 0.05 have been connected by straight line segments. *b*, The same, except that $Z^*=Z_1+\cdots+Z_7$ is the selected variable.

and introducing linear couplings, as indicated schematically in Fig. 1. The equations of the new model are

$$dX_j/dt = -q_j(Y_j^2 + Z_j^2) - a_j(X_j - F_j) + U_j \quad (1a)$$

$$dY_j/dt = X_j(q_jY_j - b_jZ_y) - p_j(Y_j - G_j) + V_j \quad (1b)$$

$$dZ_j/dt = X_j(b_jY_j + q_jZ_j) - p_jZ_j + W_j \quad (1c)$$

for $j = 1, \ldots, 2^L - 1$, where

$$U_{2_j} = -cp_jY_j \quad (2a)$$

$$U_{2j+1} = -cp_jZ_j \quad (2b)$$

$$V_j = cp_j(X_{2_j} - h_{2_j}) \quad (2c)$$

$$W_j = cp_j(X_{2_{j+1}} - h_{2_{j+1}}) \quad (2d)$$

for $j = 1, \ldots, (2^{L-1} - 1)$.

In these calculations I have let $p_j = 1.0$, $q_j = 1.0$, $a_j = 0.25$, $b_j = 4.0$, $F_j = 8.0$, $G_j = 1.0$ and $h_j = 1.0$ for all values of j, while letting the coupling coefficient c be 0.1 for 'weak' and 1.0 for 'strong' coupling. I have used the 'standard' fourth-order Runge-Kutta procedure with a time step of 0.025 units in all numerical integrations. In each application of the Grassberger-Procaccia (GP) procedure I have let τ and τ' equal 8 time steps, and, after generating a sequence of values of a selected variable, I have let $N = 4{,}000$ for various values of n. This value is typical of many of the real-world studies (although N is considerably larger in some).

For $L = 1$ the new model reduces to the three-variable model. With the indicated values of the parameters it behaves chaotically, with $d' = 2.4$. Figure 2 shows a Poincaré section of a 'reconstructed' attractor, obtained by using fourth-degree polynomial interpolation to identify a sequence of times t' at which $Z_1(t') = 0$, and then plotting values of $Z_1(t' + 2\tau)$ against values of $Z_1(t' + \tau)$. The GP procedure, with Z_1 as the selected variable, indicates a value of d_c slightly exceeding 2.0.

For $L = 3$ the indicated value of d' when $c = 0.1$ is 17.0. Figure 3a shows curves of $m(r)$ against r obtained when Z_7 is the selected variable. According to Fig. 1, Z_7 is very weakly coupled to most of the 21 variables, particularly Y_4, Z_4, Y_5 and Z_5. The central portions of the right-hand curves suggest that d_c is near 4.0, whereas the lower portions suggest a value near 5.5. One might argue that the procedure has not converged to any answer, but there is certainly no suggestion of a value comparable to

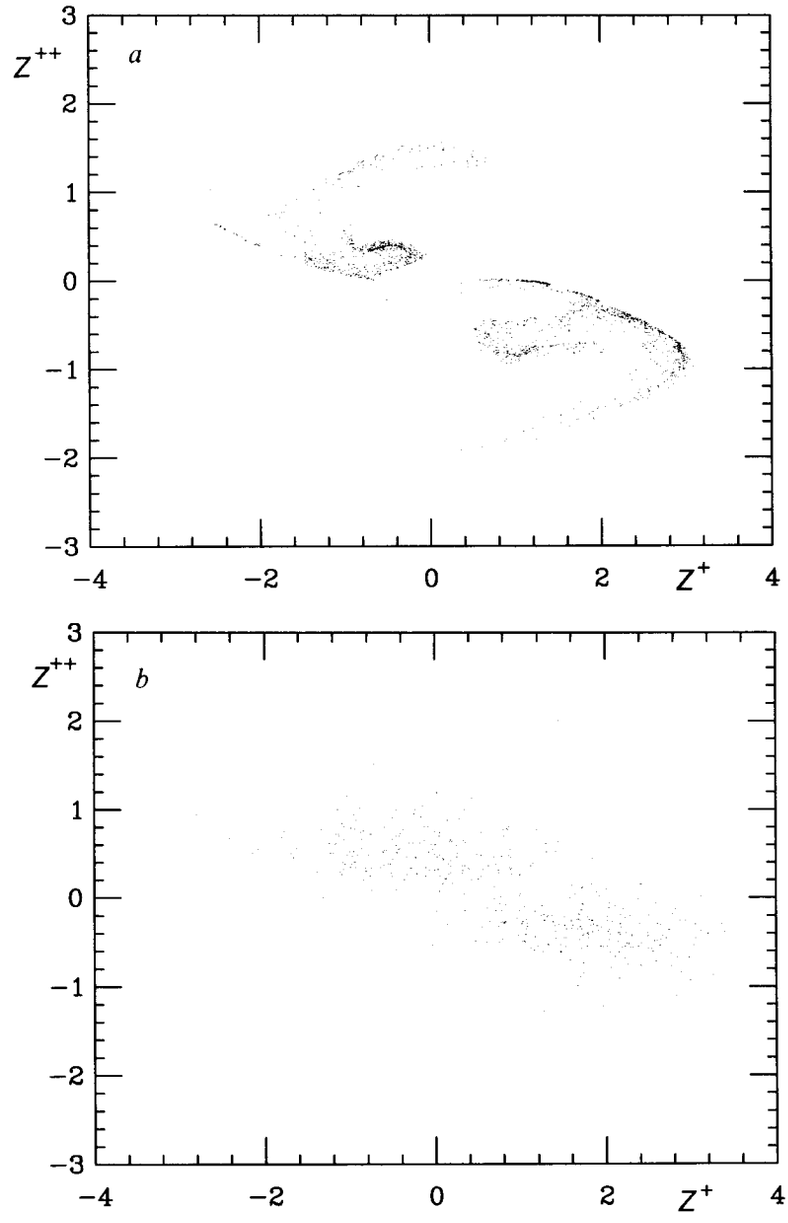

FIG. 4 *a*, Plane projection of Poincaré section of reconstructed attractor of equation (1) with $L = 3$ and $c = 0.1$, obtained by plotting $Z^{++} = Z_7(t' + 2\tau)$ against $Z^{+} = Z_7(t' + \tau)$ for times when $Z_7(t') = 0$. *b*, The same, except that $Z^{*} = Z_1 + \cdots + Z_7$ is used in place of Z_7.

d'. Presumably a high value of d_c would have been obtained with a very high value of N.

The model equations for $L=3$ could be rewritten with any 21 independent linear combinations of the original 21 variables as new variables, and the right-hand sides would still contain only quadratic, linear and constant terms, while d' and d_c should remain unaltered. In particular, two of the new variables could be Z_7 and the sum $Z^* = Z_1 + \cdots + Z_7$. We might expect Z^* to be fairly strongly coupled to most of the remaining variables.

Figure 3*b* is constructed similarly to Fig. 3*a*, but with Z^* as the selected variable. There is little resemblance between the figures. The right-hand curves suggest a value of d_c near 15.0, and hence comparable to d'. Repeating the calculations with $c=1.0$ gives qualitatively similar although less extreme results; d' is ~17.8, and d_c is estimated to be ~7.5 when Z_7 is the selected variable and ~15.0 when Z^* is selected. It thus appears, when N is not too large, that, first, different selected variables can yield different estimates of d_c, and, second, a suitably selected variable can sometimes yield a fairly good estimate.

Figures 4*a* and 4*b* are constructed similarly to Fig. 2, but for $L=3$, with values of Z_7 in Fig. 4*a* and Z^* in Fig. 4*b*. Each figure therefore presents a projection of a Poincaré section of a high-dimensional attractor on a plane. The remarkable feature is that at coarse scales Fig. 4*a* looks very much like Fig. 2, although at fine scales it is more like Fig. 4*b*. The implication is that if N is so small that the smallest value of r for which $m(r)$ is statistically meaningful is still in the coarse-scale range, the estimate of d_c for $L=3$ with Z_7 as the selected variable ought to resemble the estimate for $L=1$ when Z_1 is selected more than the one for $L=3$ when Z^* is selected.

I therefore see no reason to believe that an extensive weather or climate system possesses a low-dimensional attractor. At the same time, I do not feel that most of the real-data studies are meaningless; they merely need to be reinterpreted. As suggested in one study[5], the atmosphere might be viewed as a loosely coupled set of lower-dimensional subsystems. Perhaps the procedure, as practised, attempts to measure the dimension of a subsystem. □

Received 1 May; accepted 6 August 1991.

1. Grassberger, P. & Procaccia, I. *Phys. Rev. Lett.* **50,** 346–349 (1983); *Physica* D**3,** 189–208 (1983).
2. Fraedrich, K. *J. atmos. Sci.* **43,** 419–432 (1986).
3. Essex, C., Lookman, T. & Nerenberg, M. A. H. *Nature* **326,** 64–66 (1987).
4. Keppenne, C. L. & Nicolis, C. *J. atmos. Sci.* **46,** 2356–2370 (1989).
5. Tsonis, A. A. and Elsner, J. B. *Nature* **333,** 545–547 (1988); *Bull. Am. met. Soc.* **70,** 14–23 (1989).
6. Sharifi, M. B., Georgakakos, K. P. & Rodriguez-Iturbe, I. *J. atmos. Sci.* **47,** 888–893 (1990).
7. Fraedrich, K. & Leslie, L. M. *Q. J. R. met. Soc.* A**115,** 79–91 (1989).
8. Grassberger, P. *Nature* **323,** 609–612 (1986).
9. Nicolis, C. & Nicolis, G. *Nature* **311,** 529–532 (1984); **326,** 523 (1987).
10. Grassberger, P. *Nature* **326,** 524 (1987).
11. Procaccia, I. *Nature* **333,** 498–499 (1988).
12. Osborne, A. R. & Provenzale, A. *Physica* D**35,** 357–381 (1989).
13. Theiler, J. *J. opt. Soc. Am.* A**7,** 1055–1073 (1990).
14. Ruelle, D. *Proc. R. Soc.* A**427,** 241–248 (1990).
15. Kaplan, J. L. & Yorke, J. A. *Lect. Not. Math.* **730,** 204–219 (1979).
16. Lorenz, E. N. *Tellus* A**36,** 98–110 (1984); A**42,** 378–389 (1990).

ACKNOWLEDGEMENTS. I thank H. Abarband, R. Brown and S. Islam for their suggestions and assistance. This work was sponsored by the University Research Initiative of the Defense Advanced Research Project Agency and the Climate Dynamics Program of the NSF.

Wintertime asymmetry of upper tropospheric water between the Northern and Southern Hemispheres

K. K. Kelly*, A. F. Tuck & T. Davies†

* National Oceanic and Atmospheric Administration Aeronomy Laboratory, 325 Broadway, Boulder, Colorado 80303-3328 USA
† ECMWF, Reading, Berkshire, UK

WATER vapour is an important greenhouse gas[1–3] and yet its abundance in the upper troposphere is poorly known. Upper-tropospheric water vapour is particularly important despite its low mixing ratios, because it has large effects on the flux of infrared radiation near the tropopause[2]. In addition, the distribution and supply of water vapour are central to cloud formation; the effects of cloud on the Earth's radiation budget are in turn central to understanding the climate response to increasing atmospheric concentrations of greenhouse gases. From airborne measurements of total water (vapour plus ice crystal)[4] during the winters of 1987 in the Southern Hemisphere and of 1988–89 in the Northern Hemisphere, we find that the upper troposphere in middle, subpolar and high latitudes is a factor of 2–4 drier during austral winter than during boreal winter. As the lower-latitude air moves towards the pole in austral winter, it is forced to cool to lower temperatures than in the north—more of the water vapour therefore condenses to form ice crystals, which then precipitate, thereby removing moisture from the air mass. Clearly, climate models must be able to reproduce this asymmetry if their predictions are to be credible. We also note that the asymmetry in water vapour implies an asymmetry in the production rate of the hydroxyl radical, and hence in the tropospheric chemistry of each hemisphere, for example in the rate of methane loss[5].

During the Airborne Antarctic Ozone Experiment (AAOE) and the Airborne Arctic Stratospheric Expedition (AASE), the NASA ER-2 and DC-8 aircraft obtained many profiles of water in the upper troposphere above Punta Arenas (53° S, 71° W) and Stavanger (59° N, 6° E) during August to September 1987 and late December to February 1988/9 respectively. A lesser number of profiles was obtained at Puerto Montt (41° S, 73° W), Christchurch (44° S, 172° E), Moffett Field (37° N, 122° W) and Wallops Island (38° N, 75° W), all with the Lyman-α resonance fluorescence hygrometer[4]. The DC-8 aircraft completed more than 30 flights averaging >10 h duration on the two missions, mostly in the upper troposphere between 300 and 200 mbar. The average profile for each austral site and for each boreal site is shown in Fig. 1. For each set of three sites, the Northern Hemisphere contains a factor of 2–4 more water molecules in the upper troposphere than does the Southern Hemisphere. The relative frequencies of cloud near the tropopause at the sites have been discussed by Murphy *et al*[6]. The difference in the upper-tropospheric water content is a striking extension downwards of the inter-hemispheric asymmetry in water observed in the stratosphere[7] by the ER-2.

The large numbers of upper-tropospheric water observations obtained by the DC-8 in horizontal flight are shown in Fig. 2. Below the saturation curve the data refer to water vapour, above the curve they are the sum of vapour plus ice crystals. The asymmetry is present for both sets of data (clear air and clouds). The total water content of cloud is an important factor in cloud feedback as simulated by general circulation models[8,9]. Note also that in clear air, the extreme dry population is made up entirely of austral points, whereas the extreme moist population consists of boreal points.

We examine air motions and temperatures associated with a very cold balloon ascent from the South Pole on 24 July 1987, using air parcel trajectories calculated from the analysis data from the European centre for medium-range weather forecasts (ECMWF). The temperature and pressure data were recorded from an ozonesonde flown by NOAA/CMDL[10] and are shown in Fig. 3. It is clear from the ozonesonde that the tropopause is at ~180 mbar. This is not an unusual tropopause height over Antarctica in winter[11–13]. The saturation mixing ratio for vapour over ice on this profile is less than 5 p.p.m.v. at 300 K, a potential